Amino Acids

# Radiopharmacological characterization of 64Cu-labeled α-MSH analogs for potential use in imaging of malignant melanoma

--Manuscript Draft--

| | |
|---|---|
| **Manuscript Number:** | AMAC-D-15-00521 |
| **Full Title:** | Radiopharmacological characterization of 64Cu-labeled α-MSH analogs for potential use in imaging of malignant melanoma |
| **Article Type:** | Original Article |
| **Corresponding Author:** | Wiebke Sihver, Ph.D.<br><br>GERMANY |
| **Corresponding Author E-Mail:** | w.sihver@hzdr.de |
| **Corresponding Author Secondary Information:** | |
| **Corresponding Author's Institution:** | |
| **Corresponding Author's Secondary Institution:** | |
| **First Author:** | Feng Gao, M.S. |
| **First Author Secondary Information:** | |
| **Order of Authors:** | Feng Gao, M.S. |
| | Wiebke Sihver, Ph.D. |
| | Christoph Jurischka, B.S. |
| | Ralf Bergmann, Ph.D. |
| | Cathleen Haase-Kohn, Ph.D. |
| | Birgit Mosch, Ph.D. |
| | Jörg Steinbach, Ph.D. |
| | Davide Carta, Ph.D. |
| | Cristina Bolzati, Ph.D. |
| | Andrea Calderan, Ph.D. |
| | Jens Pietzsch, Ph.D. |
| | Hans-Jürgen Pietzsch, Ph.D. |
| **Order of Authors Secondary Information:** | |
| **Funding Information:** | German Academic Exchange Service (A/11/94299, 91540213) — Mr. Feng Gao |
| **Abstract:** | The melanocortin-1 receptor (MC1R) plays an important role in melanoma growth, angiogenesis and metastasis, and is overexpressed in melanoma cells. α-Melanocyte stimulating hormone (α-MSH) and derivatives are known to bind with high affinity at this receptor that provides the potential for selective targeting of melanoma.<br>In this study, one linear α-MSH-derived peptide Nle-Asp-His-D-Phe-Arg-Trp-Gly-NH2 (NAP-NS1) without linker and with εAhx-β-Ala linker, and a cyclic α-MSH derivative, [Lys-Glu-His-D-Phe-Arg-Trp-Glu]-Arg-Pro-Val-NH2 (NAP-NS2) with εAhx-β-Ala linker were conjugated with p-SCN-Bn-NOTA and labeled with 64Cu. Radiochemical and radiopharmacological investigations were performed with regard to transchelation, stability, lipophilicity and in vitro binding assays as well as biodistribution in healthy rats.<br>No transchelation reactions, but high metabolic stability and water solubility were |

| | |
|---|---|
| | demonstrated. The linear derivatives showed higher affinity than the cyclic one. [64Cu]Cu-NOTA-εAhx-β-Ala-NAP-NS1 ([64Cu]Cu-2) displayed rapid cellular association and dissociation in murine B16F10 cell homogenate. All [64Cu]Cu-labeled conjugates exhibited affinities in the low nanomolar range in B16F10. [64Cu]Cu-2 showed also high affinity in human MeWo and TXM13 cell homogenate. In vivo studies suggested that [64Cu]Cu-2 was stable, with about 85% of intact peptide in rat plasma at 2 h p.i. Biodistribution confirmed the renal pathway as major elimination route. The uptake of [64Cu]Cu-2 in the kidney was 5.9% ID/g at 5 min p.i. and decreased to 2.0% ID/g at 60 min p.i.<br>Due to the prospective radiochemical and radiopharmacological properties of the linear α-MSH derivative [64Cu]Cu-2 this conjugate is a promising candidate for tracer development in human melanoma imaging. |
| **Suggested Reviewers:** | Thomas L Mindt, Ph.D.<br>Scientist Leader, University Hospital Basel<br>thomas.mindt@usb.ch |

# Radiopharmacological characterization of $^{64}$Cu-labeled α-MSH analogs for potential use in imaging of malignant melanoma

Feng Gao[1,2], Wiebke Sihver[1]*, Christoph Jurischka[1,3], Ralf Bergmann[1], Cathleen Haase-Kohn[1], Birgit Mosch[1], Jörg Steinbach[1,2], Davide Carta[4], Cristina Bolzati[4], Andrea Calderan[5], Jens Pietzsch[1,2], Hans-Jürgen Pietzsch[1,2]

[1] *Helmholtz-Zentrum Dresden-Rossendorf, Institute of Radiopharmaceutical Cancer Research, Bautzner Landstraße 400, 01328 Dresden, Germany*

[2] *Technische Universität Dresden, Department of Chemistry and Food Chemistry, 01062 Dresden, Germany*

[3] *Brandenburg University of Technology Cottbus-Senftenberg, Germany*

[4] *IENI-CNR, Corso Stati Uniti 4, 35127 Padova, Italy*

[5] *ICB-CNR,Via Marzolo,1, 35131 Padova, Italy*

**Abbreviated title**: $^{64}$Cu-labeled NAPamides for melanoma imaging

**Key words**: Melanocortin-1 receptor, α-MSH analogs, $^{64}$Cu labeling, malignant melanoma

***Corresponding author**: Wiebke Sihver
w.sihver@hzdr.de
Tel *49 (0) 351 260 2424
Fax *49 (0) 351 260 3232

**Acknowledgements**

Feng Gao thanks the German Academic Exchange Service (DAAD) for financial support (A/11/94299, 91540213).

The excellent technical assistance of Regina Herrlich, Utta Herzog and Andrea Suhr is greatly acknowledged.

**Abstract**

The melanocortin-1 receptor (MC1R) plays an important role in melanoma growth, angiogenesis and metastasis, and is overexpressed in melanoma cells. α-Melanocyte stimulating hormone (α-MSH) and derivatives are known to bind with high affinity at this receptor that provides the potential for selective targeting of melanoma.

In this study, one linear α-MSH-derived peptide Nle-Asp-His-D-Phe-Arg-Trp-Gly-$NH_2$ (NAP-NS1) without linker and with εAhx-β-Ala linker, and a cyclic α-MSH derivative, [Lys-Glu-His-D-Phe-Arg-Trp-Glu]-Arg-Pro-Val-$NH_2$ (NAP-NS2) with εAhx-β-Ala linker were conjugated with p-SCN-Bn-NOTA and labeled with $^{64}$Cu. Radiochemical and radiopharmacological investigations were performed with regard to transchelation, stability, lipophilicity and in vitro binding assays as well as biodistribution in healthy rats.

No transchelation reactions, but high metabolic stability and water solubility were demonstrated. The linear derivatives showed higher affinity than the cyclic one. [$^{64}$Cu]Cu-NOTA-εAhx-β-Ala-NAP-NS1 ([$^{64}$Cu]Cu-**2**) displayed rapid cellular association and dissociation in murine B16F10 cell homogenate. All [$^{64}$Cu]Cu-labeled conjugates exhibited affinities in the low nanomolar range in B16F10. [$^{64}$Cu]Cu-**2** showed also high affinity in human MeWo and TXM13 cell homogenate. In vivo studies suggested that [$^{64}$Cu]Cu-**2** was stable, with about 85% of intact peptide in rat plasma at 2 h p.i. Biodistribution confirmed the renal pathway as major elimination route. The uptake of [$^{64}$Cu]Cu-**2** in the kidney was 5.9% ID/g at 5 min p.i. and decreased to 2.0% ID/g at 60 min p.i.

Due to the prospective radiochemical and radiopharmacological properties of the linear α-MSH derivative [$^{64}$Cu]Cu-**2** this conjugate is a promising candidate for tracer development in human melanoma imaging.

**Introduction**

Melanoma accounts for less than 2% of skin cancer but it causes a large majority of skin cancer death. If melanoma can be detected in an early stage to be removed surgically, the overall 5-year survival rate is 98%. However, it dramatically falls to 63% when lymph nodes were affected and even to 16% when metastases occur (American Cancer Society 2015).

Current clinical diagnosis of melanoma relies on the morphology of melanoma, but the diagnostic accuracy of melanoma differs from more than 77% for the superficial-spreading type down to 41% for nodular type, or only 21% for desmoplastic melanomas (Tandler et al. 2012; Lin et al. 2014).

Therefore, it is highly desired to develop effective imaging tracers for precise detection of melanoma, especially for primary metastatic melanoma. The melanocortin type 1 receptor (MC1R) is overexpressed in melanoma cells (Loir et al. 1999; Salazar-Onfray et al. 2002; López et al. 2007), and represents a distinct molecular target for malignant melanoma imaging.

Wild type α-melanocyte stimulating hormone (α-MSH) is a potent naturally occurring melanotropic peptide to activate MC1Rs, but it displays a short half-life in culture medium (Sawyer et al. 1980) and blood serum (Ashton et al. 1977; Rudman et al. 1983; Eberle 1988). The replacement of $Met^4$ and $Phe^7$ by Nle and D-Phe, respectively, in α-MSH prolonged the half-life, leading to [$Nle^4$,D-$Phe^7$]-α-MSH (NDP-MSH) that has even higher affinity than α-MSH and is more stable (Sawyer et al. 1980; Siegrist et al. 1988; Lunec et al. 1992). Even shorter linear peptides [Ac-$Nle^4$, $Asp^5$, D-$Phe^7$]-α-$MSH_{4-11}$ (NAPamides) also show high affinities in the low nanomolar range at MC1R (Froidevaux et al. 2004; Cheng et al. 2007; Bapst et al. 2007). In this regard, Froidevaux et al. (2004) conjugated the metal chelator DOTA to the ε-amino group of the C-terminal lysine ($Lys^{11}$) of NAPamide (DOTA-NAPamide) and radiolabeled with $^{111}$In and $^{67}$Ga/$^{68}$Ga. Both $^{111}$In-DOTA-NAPamide and $^{67}$Ga-DOTA-NAPamide exhibited high tumor accumulation, indicating that modification to the terminal $Lys^{11}$ did not compromise receptor affinity, and low kidney uptake leading to high tumor-to-kidney ratios (Froidevaux et al. 2004, 2005). In another study, Cheng et al. (2007) radiolabeled DOTA-NAPamide with $^{64}$Cu and found that [$^{64}$Cu]Cu-DOTA-NAPamide showed high accumulation in tumors, but the radioactivity levels in liver and kidney were relatively high. It is suggested that the high hepatobiliary radioactivity accumulation was primarily caused by instability of [$^{64}$Cu]Cu-DOTA coordination in vivo (Cheng et al. 2007). Nevertheless, NAPamides are proposed to be interesting agents for targeting melanoma. Besides, it has been shown that cyclic α-MSH peptides also have high binding affinity to

MC1Rs and better resistance to proteolysis (Castrucciet al. 1984; Giblin et al. 1998; Cheng et al. 2004; Fung and Hruby 2005; Guo et al. 2009). There are several cyclization methods: cyclization via disulfide bonds (Chen et al. 2001), cyclization via metal coordination (Giblin et al. 1998; Chen et al. 2000) and cyclization via lactam bridges (Chen et al. 2001; Chen et al. 2002; Raposinho et al. 2008; Miao et al. 2008). Lactam cyclized peptides are of great interest since an improvement of both, in vivo stability and melanoma tumor uptake has been demonstrated. A lactam-cyclized α-MSH analog, based on the sequence of melanotan II has been prepared and conjugated with a pyrazolyldiamine backbone chelator. The conjugate was radiolabeled with $^{99m}$Tc-tricarbonyl and the radiolabeled complex displayed higher tumor uptake than its linear counterpart in the B16F1 melanoma mouse model. However, the clearance from the liver and kidney as well as the overall excretion rate were negatively affected by cyclization (Raposinho et al. 2008).

A different order of amino acids in receptor-targeting peptides can alter lipophilicity, radiolabeling chemistry, and linkers could affect the pharmacokinetic profiles (Schottelius and Wester 2009). The introduction of a linker between a radionuclide in a bifunctional chelator (BFC) complex and a peptide also can influence the physicochemical properties of the radiolabeled peptide, causing steric effects of the chelator on the binding affinity to the receptors and thus modifying the pharmacokinetic profile such as clearance rate from the kidney (Yang et al. 2010; Fani and Maecke 2012).

In the present study, NAPamide analogs with and without ε-Ahx-β-Ala linker (indicated as β-Ala) NAP-NS1 (no linker) and NAP-NS1-β-Ala were used. These two linear peptides together with the cyclic peptide NAP-NS2-β-Ala were studied as agents to target the MC1R. p-SCN-Bn-NOTA was the chelator coupled to the peptides because it forms a stable complex with copper(II) (Cooper et al. 2012). The radiopharmacological behavior of these $^{64}$Cu-labeled peptides was investigated, and the most promising one was selected for studies on human melanoma cells with regard to further investigations on appropriate mouse xenograft models.

## Materials and Methods

### *Chemicals and reagents*

$^{64}$Cu was produced at the Helmholtz-Zentrum Dresden-Rossendorf by a biomedical cyclotron (Cyclone 18/9, IBA, Louvain la Neuve, Belgium). Two linear peptides NAP-NS1 (no linker; Nle-Asp-His-D-Phe-Arg-Trp-Gly-$NH_2$) and NAP-NS1-β-Ala (with β-Ala linker; ε-Ahx-β-Ala-Nle-Asp-His-D-Phe-Arg-Trp-Gly-$NH_2$) as well as one cyclic peptide NAP-NS2-β-Ala (with β-Ala linker; ε-Ahx-β-Ala-Lys-Glu-His-D-Phe-Arg- Trp-Glu-Arg-Pro-Val-$NH_2$, cyclized from $Lys^3$ to $Glu^9$) were custom made by GL Biochem, Shanghai, Ltd following the previously reported procedure from Biondi et al. (2010). p-NOTA-Bn-SCN (NOTA) was purchased from Macrocyclics, Inc., USA. ($Nle^4$, D-$Phe^7$)-α-MSH (NDP-MSH) was purchased from Bachem AG, Switzerland. [$^{125}$I]I-NDP-MSH was obtained from Biotrend Chemikalien GmbH, Germany. All other chemical and biological reagents were purchased from Sigma Aldrich, USA, and Biochrom AG, Germany, respectively. Semi-preparative high-performance liquid chromatography (HPLC) was carried out on a chromatography system equipped with a Perkin Elmer UVIVIS LC290 UV detector and a flow-through radioactivity detector (Raytest Ramona) to purify and analyze the conjugates. Zorbax C18 column with inner diameter of 8 mm was used. The mobile phase was solvent A: water with 0.1% trifluoroacetic acid (TFA) and solvent B: acetonitrile with 0.1% TFA. The HPLC gradient was 0-30 min 95%-50% solvent A, 30-35 min 50% A, 35-36 min 50%-95% A, 36-41 min 95% A with a flow rate of 3 mL/min. Radioactive samples were counted using 1480 WIZARD 3" automatic gamma counter (PerkinElmer, Inc., USA). Electrospray ionization-mass spectrometry (ESI-MS) was carried out with micromass tandem quadrupole mass spectrometer (Waters Corporation, USA).

### *Preparation and (radio)chemical characterization of [$^{64}$Cu]Cu-NOTA-peptide conjugates*

***NOTA peptides conjugates*** 10 nmol of p-SCN-Bn-NOTA, 10 nmol of the native peptides (NAP-NS1, NAP-NS1-β-Ala and NAP-NS2-β-Ala) and 100-150 nmol triethylamine (TEA) in dimethylformamide (DMF) was mixed and incubated at 20°C overnight. Afterwards, 100 µL water was added to quench the reaction. The products NOTA-NAP-NS1 (**1**), NOTA-NAP-NS1-β-Ala (**2**) and NOTA-NAP-NS2-β-Ala (**3**) were purified by semi-preparative HPLC and identified by ESI-MS.

***$^{64}$Cu-labeling of the NOTA-peptides*** 1-2 nmol of **1**, **2** or **3,** dissolved in 100 µL $H_2O$, was mixed with [$^{64}$Cu]$CuCl_2$ (40-80 MBq) in 400 µL 0.2 M 2-(*N*-morpholino) ethanesulfonic acid (MES) buffer (pH 6.2) and incubated at 50°C for 20 min. Thereafter, the mixture was separated by semi-preparative

HPLC to get purified radiotracers with high specific activity. [$^{64}$Cu]Cu-NOTA-peptides isolated from semi-preparative HPLC were concentrated with a RP-18 cartridge and washed with 2 mL ethanol/$H_2O$ (v/v 1/1). The ethanol was removed by $N_2$. The radiochemical purities (RCPs) of [$^{64}$Cu]Cu-NOTA-peptides were also monitored by semi-preparative HPLC.

***Preparation of non-radioactive $^{nat}$Cu-NOTA-peptide conjugates*** 5-7.5 µmol $Cu(NO_3)_2$ x 2 $H_2O$ in 300 µL water was mixed with 5 µmol **1**, **2** or **3** in 500 µL 0.2 M MES buffer (pH 6.2) (ratio of $Cu(NO_3)_2$ x 2 $H_2O$ to NOTA-peptides 1-1.5/1) and shaked under 1000 rpm at 50°C for 60 min. Thereafter, $^{nat}$Cu-NOTA-NAP-NS1 ($^{nat}$Cu-**1**), $^{nat}$Cu-NOTA-NAP-NS1-β-Ala ($^{nat}$Cu-**2**) and $^{nat}$Cu-NOTA-NAP-NS2-β-Ala ($^{nat}$Cu-**3**), were purified by semi-preparative HPLC and characterized by ESI-MS or Maldi-MS.

***Challenge experiments*** 100 µL of [$^{64}$Cu]Cu-**1**/MES ([$^{64}$Cu]Cu-**2**/MES or [$^{64}$Cu]Cu-**3**/MES) was added to 400 µL histidine or cysteine solution (final concentration 2 nM and 0.2 nM). The mixture was vortexed and incubated at 37°C for 1 h and 24 h. Aliquots of the reaction mixture were taken and analyzed by semi-preparative HPLC.

***Stability measurements in phosphate buffer and human serum*** 100 µL of [$^{64}$Cu]Cu-**1**/MES ([$^{64}$Cu]Cu-**2**/MES or [$^{64}$Cu]Cu-**3**/MES) was mixed in 300 µL phosphate buffer (pH 7.4) or 300 µL human serum. After 1 h or 24 h of incubation at 37°C, the buffer samples were analyzed by semi-preparative HPLC. The serum samples were first treated with ethanol (twice the volume of the mixture) and centrifuged at 4°C for 30 min (13,200 rpm). The liquid phase was filtrated with the filter (VWR sterile syringe filter, 0.2 µm PES) and the filtrate was analyzed by semi-preparative HPLC.

***Determination of lipophilicity.*** 20µL of [$^{64}$Cu]Cu-**1**/MES ([$^{64}$Cu]Cu-**2**/MES or [$^{64}$Cu]Cu-**3**/MES) (0.2 MBq) was diluted in 500 µL of 1 M HEPES buffer (pH=7.4). 500 µL of n-octanol was added and the mixture stirred vigorously at 23°C for 30 min. Subsequently, the mixture was centrifuged at 23°C for 30 min (14,000 *g*) 450 µL of both water and n-octanol phases were taken and centrifuged again. The radioactivity of 100 µL of both the HEPES buffer phase and the octanol phase was measured in a gamma counter and the octanol/water partition coefficient (Log $D_{o/w}$) was calculated. The experiments were performed three times.

***Radiopharmacological assays***

Binding assays were assessed using cell homogenate of murine melanoma cell line B16F10 (ATCC® CRL-6475™), and two human melanoma cell lines MeWo (ATCC® HTB-65™) and TXM13

(University of Texas, M.D. Anderson Cancer Center, Houston, USA), as well as the MC1-receptor negative control human embryonic kidney cell line HEK-293 (ATCC® CRL-1573™). The cells were grown as monolayer at 37°C in a humidified atmosphere comprising 5% $CO_2$ and 95% air in DMEM medium including 10% FCS (Biochrom AG). After washing the confluent cells twice with phosphate buffered saline (PBS) and detaching them with trypsin/EDTA (0.05%/0.02%), the cells were suspended in DMEM and homogenized (Potter-Elvehjem) by forcing 20 times the pestle up and down the rounded vessel on ice. The assays were performed in a final volume of 200 µL.

***Competition assay*** In vitro binding affinity of the non-radiolabeled peptides was assessed in competition binding assays using B16F10 and MeWo cell homogenate and [$^{125}$I]I-NDP-MSH as standard radioligand. Homogenized cells were incubated with 40 µL [$^{125}$I]I-NDP-MSH (final concentration 0.2 nM) in the presence of increasing concentrations of the three native peptides, **1**, **2**, **3** and $^{nat}$Cu-**1**, $^{nat}$Cu-**2**, $^{nat}$Cu-**3** (final concentrations $5.01\times10^{-14}$ to $2.45\times10^{-6}$ M for B16F10; $5.01\times10^{-14}$ to $1.23\times10^{-6}$ M for MeWo), as well as for comparison NDP-MSH ($10^{-14}$ to $2.45\times10^{-5}$ M) at 23°C for 90 min.

***Kinetic assay*** [$^{64}$Cu]Cu-**2** was selected to conduct a kinetic study in homogenized B16F10 cells. The association rate was evaluated starting the incubation with [$^{64}$Cu]Cu-**2** (final concentration 8 nM) in reverse order (120, 90, 60, 30, 20, 10 and 5 min) at 23°C and simultaneously terminating the incubation of all samples at time 0. In adjacent samples dissociation was initiated by adding 610 µM of NDP-MSH.

***Saturation binding assay*** B16F10 and HEK-293 cell homogenate was incubated with increasing concentrations of [$^{64}$Cu]Cu-**1**, [$^{64}$Cu]Cu-**2** and [$^{64}$Cu]Cu-**3** (0.1 nM to 10 nM for [$^{64}$Cu]Cu-**2** on B16F10 and TXM13 cells, for [$^{64}$Cu]Cu-**1** on B16F10 cells; 0.2 nM to 20 nM for [$^{64}$Cu]Cu-**3** on B16F10 cells, for [$^{64}$Cu]Cu-**2** on MeWo cells; 0.01 nM to 1 nM for [$^{125}$I]I-NDP-MSH on B16F10 and TXM13 cells; 0.02 nM to 2 nM for [$^{125}$I]I-NDP-MSH on MeWo cells). Thus, MeWo and TXM13 cell homogenate was incubated only with [$^{64}$Cu]Cu-**2**. The three cell lines were incubated with [$^{125}$I]I-NDP-MSH (0.016 to 2 nM) for comparison at 23°C for 90 min; adjacent samples received additionally 610 µM of NDP-MSH to obtain the nonspecific binding.

The incubation of all samples was stopped by washing the homogenate with cold PBS four times using a filter (Whatman GF/C, 90 min presoaked in 0.3% polyethyleneimine) in a cell harvester (Brandel, USA). The radioactivity bound to the filter was measured in a gamma counter. In adjacent samples

without cell homogenate the pure filter binding was determined. The experiments were performed three times in triplicates. Pharmacological paramaters as association and dissociation half time, inhibitory constants ($K_i$), dissociations constants ($K_d$) and maximal binding capacities ($B_{max}$) were calculated by fitting the data using a nonlinear curve fitting program (GraphPad Prism 5.02). The data fitted best to a one-binding-site-model. Determination of protein content of the cell samples from the saturation assays with the bicinchoninic acid (BCA) protein assay kit (Pierce, Thermo Scientific) was used to calculate $B_{max}$ in fmol/mg.

***In vivo metabolic assay and biodistribution***

The animal experiments were performed in accordance to the guidelines of the German Regulationsofr Animal Welfare. The protocol was approved by the local Ethical Committee for Animal Experiments (reference number 24-9168.21-4/2004-1).

Wistar rats (Wistar Unilever, HsdCpb: Wu, Harlan Winkelmann GmbH, Borchen, Germany) were housed under standard conditions with free access to standard food and tap water.

For biodistribution of [$^{64}$Cu]Cu-**2** two groups of rats (n = 8 each) were sacrificed under desfluorane anesthesia at 5 and 60 min, respectively, after injection of 0.30 ± 0.03 MBq (500 µL). Organs and tissues of interest were removed, and weighed, and the radioactivity was measured in a cross-calibrated well counter (WIZARD, Automatic Gamma Counter, Perkin Elmer, Waltham, MA, USA) or dose calibrator (Aktivimeter Isomed 2000; MED-Nuklear-Medizintechnik, Dresden, Germany). The decay corrected data were normalized to the amount of injected activity calculated from the activity of injection syringes before and after injection and expressed as percentage of injected activity (%ID) or standardized uptake values (SUV = ratio of radioactivity per weight of tissue to injected radioactivity per rat body weight). Values are quoted as mean ± standard deviation (mean ± SD) for one group of animals.

For metaboltite studies male Wistar rats (n = 4; body weight 180 ± 20 g) were anesthetized with desflurane (9-10%, 30% oxygen/air). The threshold value for breathing frequency was 65 breaths/min. Animals were put in supine position and placed on a heating pad to maintain body temperature. The spontaneously breathing rats were heparinized with 100 units/kg heparin (Heparin-Natrium 25.000-ratiopharm®, ratiopharm GmbH, Germany) by subcutaneous injection to prevent blood clotting on intravascular catheters. After local anesthesia with lignocaine (1%, Xylocitin®loc, mibe, Jena, Germany) into the right groin, a catheter (0.8 mm Umbilical Vessel Catheter, Tyco Healthcare,

Tullamore, Ireland) was introduced into the right femoral artery for arterial blood sampling. A second needle catheter (35G) was placed into a tail vein and was used for [$^{64}$Cu]Cu-**2** injection (15 MBq in 500 µL of infusions solution with 5 % ethanol). For metabolic analysis, arterial blood samples were taken 2.5, 5, 10, 20, 30, 60 and 120 min after injection. Arterial plasma was separated by centrifugation (10 min at 1,300 × *g*) followed by precipitation of the proteins with methanol (2 volumes to 1 volume plasma) followed by 5 min storage at -60°C. The clear supernatant separated by centrifugation was used for analysis. The radio-HPLC system (Agilent 1100 series) applied for metabolite analysis was equipped with UV detection (254 nm) and an external radiochemical detector (RAMONA, Raytest GmbH, Straubenhardt, Germany). Analysis was performed on a Zorbax C18 300SB (250 × 9.4 mm; 4 µm) column with an eluent system A ($H_2O$ + 0.1% TFA) and B (acetonitrile + 0.1% TFA).

**Results**

***Preparation and (radio)chemical characterization of the NOTA-peptide conjugates***

***Preparation and characterization of NOTA-peptides conjugates*** The NOTA-peptides **1**, **2** and **3** were synthesized with chemical yields of 42%, 35% and 21%, respectively. They were characterized by ESI-MS or Maldi-TOF-MS. **1**: 1380.44 $[M+H]^+$ (measured data), 1379.54 (calculated data); **2**: 1564.38 $[M+H]^+$, 782.64 $[M+2H]^{2+}$ (measured data), 1563.78 (calculated data); **3**: 1001.83 $[M+2H]^{2+}$, 667.38 $[M+3H]^{3+}$ (measured data), 1999.30 (calculated data).

***Radiochemistry*** NOTA-conjugated peptides were readily labeled with $^{64}$Cu at 50°C for 20 min. The chemical structures of the [$^{64}$Cu]Cu-labeled peptides are sketched in **Fig**. **1**. In each case, the reaction was followed by RP-HPLC with sequential UV and radiodetection.

After purification, the radiochemical purities of [$^{64}$Cu]Cu-**1** and [$^{64}$Cu]Cu-**2** were over 95%, and the specific activities ranged from 14-30 GBq/µmol.

**Fig. 1** Chemical structures of the [$^{64}$Cu]Cu-NOTA-conjugates. **a**) [$^{64}$Cu]Cu-**1**; **b**) [$^{64}$Cu]Cu-**2**; **c**) [$^{64}$Cu]Cu-**3**

To confirm the chemical identity of the radiolabeled compounds, the corresponding $^{nat}$Cu-compounds were prepared at millimolar level by reacting in MES buffer at 50°C for 60 min, $Cu(NO_3)_2$ x 2 $H_2O$ with the selected NOTA-peptide in 1-1.5/1 ratio. Compounds were purified by semi-preparative HPLC and characterized by ESI-MS or Maldi-TOF-MS analyses. After purification the yields for $^{nat}$Cu-**1**,

$^{nat}$Cu-**2** and $^{nat}$Cu-**3** were 41%, 33% and 19%, respectively. The mass spectra showed the expected signals consistent with the formula referable to the complexes: $^{nat}$Cu-**1**: 1440.63/1442.78 $[M+H]^+$, 721.79/720.89 $[M+2H]^{2+}$ (measured data), 1440.07 (calculated data); $^{nat}$Cu-**2**: 1625.72 $[M+H]^+$, 813.09/814.63 $[M+2H]^{2+}$ (measured data), 1624.69 (calculated data); $^{nat}$Cu-**3**: 2063.69 $[M+H]^+$ (measured data), 2061.84 (calculated data). were used to confirm the [$^{64}$Cu]Cu-**1**, [$^{64}$Cu]Cu-**2** and [$^{64}$Cu]Cu-**3**. **Fig**. **2** shows HPLC analyses of the $^{nat}$Cu-compounds (UV) compared with those of the corresponding $^{64}$Cu labeled peptides (radiometric). The chromatographic profile displayed superimposable UV and radiometric peaks. Notably, at tracer level, upon the $^{64}$Cu-coordination two distinct isomers were observed for $^{64}$Cu-labeled linear NOTA-peptides (**Fig**. **2** [$^{64}$Cu] Cu-**1** and [$^{64}$Cu]Cu-**2**) (Schlesinger et al. 2011).

For both [$^{64}$Cu]Cu-**1** and [$^{64}$Cu]Cu-**2** peptides, in HPLC analysis the first isomer appeared about 1.5 ± 0.5 min earlier than the second one, major isomer. On [$^{64}$Cu]Cu-**2**, the conversion of the isomers was investigated. The second isomer was isolated and immediately analized by HPLC. Only one peak corresponding to the major isomer was observed. Injecting 10 min later two isomers were found, in a 1:10 ratio. Since the isomers equilibrate so fast they were not separated from each other.

**Fig. 2** Chromatograms of $^{64}$Cu-labeled NOTA-peptides (radioactivity detection) and corresponding non-radioactive reference compounds (UV detection). All HPLC runs are performed under the same condition with the same HPLC device

***Challenge study*** An excess of free histidine or cysteine to the $^{64}$Cu-labeled peptides yielded in nearly no transchelation reaction. Detection of 94% (histidine) and 93% (cysteine) of intact [$^{64}$Cu-labeled peptides after 24 h challenge with 1 mM and 10 mM histidine or cysteine, respectively, might imply negligible transchelation.

***Stability study in buffer and human serum*** The stability in phosphate buffer was >99% for [$^{64}$Cu]Cu-**2** and [$^{64}$Cu]Cu-**3** after 24 h, and for [$^{64}$Cu]Cu-**1** about 98% after 24 h. In serum >98% of the $^{64}$Cu-labeled peptides was measured, only for [$^{64}$Cu]Cu-**1** about 97% after 24h, indicating that [$^{64}$Cu]Cu-**1**, [$^{64}$Cu]Cu-**2** and [$^{64}$Cu]Cu-**3** were sufficiently stable both in buffer and serum.

***Determination of lipophilicity***. The log $D_{o/w}$ values for [$^{64}$Cu]Cu-**1**, [$^{64}$Cu]Cu-**2** and [$^{64}$Cu]Cu-**3** obtained by the "shake flask" method under physiological conditions resulted in -2.55 ± 0.035, -2.30 ± 0.00 and -3.39 ± 0.04, respectively, demonstrating the hydrophilic nature of the three radiolabeled

peptides. The cyclic conjugate [$^{64}$Cu]Cu-**3** displayed a little higher hydrophilic character compared to [$^{64}$Cu]Cu-**1** and [$^{64}$Cu]Cu-**2**.

It is worth noting that despite the high hydrophilicity the labeled peptides showed a high tendency to stick to the wall of vials or injection syringes. To avoid the adsorption phenomenon, after evaporation of the elution solvent [$^{64}$Cu]Cu-**1**, [$^{64}$Cu]Cu-**2** and [$^{64}$Cu]Cu-**3** were dissolved in MES buffer (pH=7.0) containing 10% ethanol.

***Radiopharmacological assays***

***Competition*** In B16F10 cell homogenate, the $K_i$ values for the three native peptides, **1**, **2**, **3** and $^{nat}$Cu-**1**, $^{nat}$Cu-**2**, $^{nat}$Cu-**3**, and in MeWo cell homogenate the $K_i$ values for NAP-NS1-β-Ala, **2** and $^{nat}$Cu-**2**, each in relation to the standard NDP-MSH, were evaluated by competition binding assays using [$^{125}$I]I-NDP-MSH. Applying the $K_d$ values of saturation assays with [$^{125}$I]I-NDP-MSH of 0.19 ± 0.01 nM and 0.23 ± 0.03 nM in B16F10 and MeWo homogenate, respectively, into the Cheng-Prusoff equation, the $K_i$ values were determined (**Table 1**).

**Table 1** $K_i$ values of the three native peptides, **1**, **2**, **3** and $^{nat}$Cu-**1**, $^{nat}$Cu-**2**, $^{nat}$Cu-**3** and NDP-MSH on B16F10 and MeWo cell homogenate (mean ± SEM of three assays)

| **B16F10** | | | | | | |
|---|---|---|---|---|---|---|
| | | $K_i$ (nM) | NOTA | $K_i$ (nM) | $^{nat}$Cu-NOTA | $K_i$ (nM) |
| Linear no linker | NAP-NS1 | 0.5 ± 0.1 | **1** | 0.7 ± 0.2 | $^{nat}$Cu-**1** | 0.5 ± 0.02 |
| Linear β-Ala | NAP-NS1-β-Ala | 0.5 ± 0.1 | **2** | 1.2 ± 0.1 | $^{nat}$Cu-**2** | 3.5 ± 0.5 |
| Cyclic β-Ala | NAP-NS2-β-Ala | 12 ± 1 | **3** | 81 ± 4 | $^{nat}$Cu-**3** | 138 ± 9 |
| | NDP-MSH | 0.01 ± 0.00 | | | | |
| **MeWo** | | | | | | |
| Linear β-Ala | NAP-NS1-β-Ala | 1.2 ± 0.1 | **2** | 1.5 ± 0.1 | $^{nat}$Cu-**2** | 4.6 ± 0.2 |
| | NDP-MSH | 0.7 ± 0.1 | | | | |

In general, the affinity of the standard compound NDP-MSH ($K_i$ 0.01 ± 0.00 nM) to MCR1 was considerably higher than that of the investigated peptides.

In B16F10 cells, the linear peptides (NAP-NS1, NAP-NS1-β-Ala, **1**, **2**, $^{nat}$Cu-**1**, $^{nat}$Cu-**2**) showed higher affinities with respect to the cyclic peptide conjugates (**Fig. 3**). Indeed, NAP-NS2-β-Ala, 3, $^{nat}$Cu-3 exhibit a considerably decrease of the receptor affinity, with $K_i$ values of 12 nM, 81 nM and 138 nM,

respectively. In all cases, the NOTA coupling and the metalation with $^{nat}$Cu lead to a reduction of the receptor affinity; this was particularly evident for NAP-NS2-β-Ala peptide. Among the linear peptides, the NOTA derivate (**2)** and the Cu-compound ($^{nat}$Cu-**2)** revealed a slight reduction of the affinity with respect to NAP-NS1-β-Ala, with $K_i$ values of 1.2 nM and 3.5 nM.

**Fig. 3** Representative competition curves of the three native peptides; **1, 2, 3** and $^{nat}$Cu-**1**, $^{nat}$Cu-**2**, $^{nat}$Cu-**3**,and NDP-MSH versus [$^{125}$I]I-NDP-MSH binding, **a)** on B16F10: ▲ NAP-NS1, △ NAP-NS1-β-Ala, ● NAP-NS2-β-Ala, ○ NDP-MSH; **b)** on B16F10: ▲ **1**, △ **2**, ● **3**, ○ $^{nat}$Cu-**1**, ◇ $^{nat}$Cu-**2**, ∗ $^{nat}$Cu-**3**; **c)** on MeWo cells: ▲ NAP-NS1-β-Ala, △ 2, ● $^{nat}$Cu-**2**, ○ NDP-MSH. Each data point arises from 3 samples. Each curve is representative for 4 assays

For investigation in MeWo human melanoma cells the linear peptides NAP-NS1-β-Ala, **2** and $^{nat}$Cu-**2** were applied and data compared with those of the standard peptide NDP-MSH ($K_i$ value of 0.73 ± 0.08 nM, **Fig. 3c**). NAP-NS1-β-Ala, **2** and $^{nat}$Cu-**2** compounds showed a high receptor affinity. Notably, in MeWo cells, the affinity of both NDP-MSH and the new investigated compounds was somewhat lower than that in murine B16F10 cells (**Table 1**).

***Kinetic assays*** To determine kinetic binding characteristics [$^{64}$Cu]Cu-**2** was selected for association and dissociation assays on B16F10 cells. **Fig. 4** illustrates a fast association and dissociation time course of [$^{64}$Cu]Cu-**2** with association and dissociation times of about 20 min. After 60 min about 90% of maximal [$^{64}$Cu]Cu-**2** binding was achieved. After association, the dissociation of [$^{64}$Cu]Cu-**2** binding was initiated by addition of NDP-MSH. Nonspecific binding was about 20%. The association and dissociation half-life was 19.4 min and 12.6 min, with an association constant ($K_{on}$) of 0.0358 $nM^{-1}min^{-1}$ and a dissociation constant ($K_{off}$) of 0.0552 $min^{-1}$, respectively. According to the equation $K_d = K_{off}/K_{on}$, a resulting $K_d$ of 1.54 nM for [$^{64}$Cu]Cu-**2** in B16F10 cells was determined. The calculated $K_d$ value of [$^{64}$Cu]Cu-**2** to B16F10 cells matched well the $K_d$ value from the saturation assays ($K_d$ 1.74 nM).

**Fig. 4** Association and dissociation of [$^{64}$Cu]Cu-**2** binding in homogenized B16F10 cells. After association of 2 h, dissociation was induced by addition of NDP-MSH (final concentration: 6.1 µM) (arrow) and followed up another 2 h. The curve represents one of three independent experiments. Data are mean of triplicates ± SD

***Saturation binding assay*** **Fig. 5** shows typical saturation graphs, obtained incubating [$^{64}$Cu]Cu-**1**, [$^{64}$Cu]Cu-**2** and [$^{64}$Cu]Cu-**3** in homogenates of B16F10, and [$^{64}$Cu]Cu-**2** in MeWo and TXM13 cells. Results were compared to those obtained with the standard [$^{125}$I]I-NDP-MSH peptide.

**Fig. 5** Representative graphs of the saturation assays **a)** of [$^{64}$Cu]Cu-**1** (left), [$^{64}$Cu]Cu-**2** (middle), [$^{64}$Cu]Cu-**3** (right) on B16F10 cells, **b)** of [$^{64}$Cu]Cu-**2** on MeWo (left) and TXM13 (right) cells, and **c)** of [$^{125}$I]I-NDP-MSH on B16F10 (left), MeWo (middle) and TXM13 (right) cells. ▲ total binding, △ nonspecific binding, ● specific binding. Each curve is representative for three independent experiments

For each compound, the $K_d$ and $B_{max}$ values are presented in **Table 2**. In murine B16F10 cells, the novel $^{64}$Cu-labeled NAPamides showed high receptor affinity with $K_d$ values in the nanomolar range. For [$^{64}$Cu]Cu-**2**, data collected in human melanoma MeWo and TXM13 cells, show $B_{max}$ values lower than those obtained in the murine melanoma cell line. In all the cell lines, the affinity of [$^{125}$I]I-NDP-MSH was somewhat higher.

On B16F10 homogenate, the nonspecific binding of the compounds, determined at $K_d$ concentrations, was <10% for [$^{64}$Cu]-**1**, [$^{64}$Cu]-**2** and [$^{125}$I]I-NDP-MSH and in the range of 30-45% for [$^{64}$Cu]-**3**. Meanwhile, on MeWo and TXM13 cells, the nonspecific for [$^{64}$Cu]-**2** and [$^{125}$I]I-NDP-MSH was in the range 30-45% (**Fig. 5**). Furthermore, assays with [$^{64}$Cu]-**1**, [$^{64}$Cu]-**2** and [$^{64}$Cu]-**3**, as well as [$^{125}$I]I-NDP-MSH using the MC1 receptor-negative cell line HEK-293 revealed no specific binding.

**Table 2** Binding parameter of [$^{64}$Cu]Cu-**1**, [$^{64}$Cu]Cu-**2** and [$^{64}$Cu]Cu-**3** on homogenate of B16F10, MeWo and TXM13 cells (mean ± SEM of three assays)

| Cell line | **B16F10** | | **MeWo** | | **TXM13** | |
|---|---|---|---|---|---|---|
| | $K_d$ (nM) | $B_{max}$ (fmol/mg) | $K_d$ (nM) | $B_{max}$ (fmol/mg) | $K_d$ (nM) | $B_{max}$ (fmol/mg) |
| [$^{64}$Cu]-**1** | 0.6 ± 0.2 | 83 ± 10 | | | | |
| [$^{64}$Cu]-**2** | 1.7 ± 0.2 | 47 ± 4 | 2.6 ± 0.4 | 17 ± 2 | 1.8 ± 0.7 | 32 ± 2 |
| [$^{64}$Cu]-**3** | 2.1 ± 0.2 | 21 ± 2 | | | | |
| [$^{125}$I]I-NDP-MSH | 0.2 ± 0.01 | 37 ± 9 | 0.2 ± 0.03 | 1.4 ± 0.1 | 0.3 ± 0.1 | 8.0 ± 1.6 |

***Biodistribution and in vivo stability***

Biodistribution and metabolism studies of [$^{64}$Cu]Cu-**2** were performed using male Wistar rats, in order to have a first insight into its potential relevance as a radiotracer for in vivo imaging of melanoma. The biodistribution data of [$^{64}$Cu]Cu-**2** are presented in **Table 3**. The data were obtained at 5 min and 60 min p.i, after intravenous bolus injection of the radiotracer. 5 min after injection high uptake values were obtained for kidney and intestine, moderately high for lung, blood and hair / skin (see also **Fig. 6**). The other organs show rather low uptake. 60 min after injection, the uptake in the organs decreased,

except for the uptake in the intestine. However, the addition of the uptake from kidney and urine is definitely higher compared to uptake of liver and intestine, already 5 min p.i, but more than twice at high 60 min p.i. showing clearly the excretion pathway via the kidney (**Fig. 6c**).

**Table 3** Biodistribution data after injection of 0.3 ± 0.03 MBq of [$^{64}$Cu]Cu-**2** (500 µL) in desfluorane anesthetized Wistar rats, 5 min and 60 min p.i., respectively. Data are expressed as standard uptake value (SUV = ratio of measured radioactivity per tissue weight to injected radioactivity per rat body weigh) after i.v. injection of 0.3 ± 0.03 MBq [$^{64}$Cu]Cu-**2** (500 µL), presented as mean of 8 rats from each group ± SD

| Organ | 5 min p.i. | 60 min p.i. |
|---|---|---|
| Brain | 0.06 ± 0.01 | 0.01 ± 0.00 |
| Pancreas | 0.62 ± 0.20 | 0.16 ± 0.06 |
| Spleen | 0.54 ± 0.22 | 0.13 ± 0.04 |
| Adrenals | 0.83 ± 0.17 | 0.22 ± 0.08 |
| Kidneys | 6.50 ± 1.37 | 2.13 ± 0.43 |
| Heart | 0.78 ± 0.10 | 0.13 ± 0.02 |
| Lung | 1.19 ± 0.13 | 0.22 ± 0.03 |
| Thymus | 0.57 ± 0.14 | 0.12 ± 0.04 |
| Thyroid* | 0.07 ± 0.01 | 0.01 ± 0.00 |
| Liver | 0.74 ± 0.15 | 0.18 ± 0.02 |
| Femur | 0.59 ± 0.07 | 0.13 ± 0.05 |
| Intestine* | 3.74 ± 0.75 | 7.42 ± 1.35 |
| Stomach* | 0.83 ± 0.17 | 0.51 ± 0.35 |
| Blood | 1.46 ± 0.14 | 0.24 ± 0.05 |
| Hair/ Skin | 1.39 ± 0.16 | 0.28 ± 0.03 |
| Muscle | 0.57 ± 0.18 | 0.14 ± 0.11 |
| Testes | 0.39 ± 0.07 | 0.14 ± 0.04 |

*for this organs %ID/g tissue was determined.

**Fig. 6** Biodistribution after injection of 0.3 ± 0.03 MBq of [$^{64}$Cu]Cu-**2** (500 µL) in desfluorane anesthetized Wistar rats, **a)** 5 min p.i., **b)** 60 min p.i. Data are expressed in mean SUV ± SD (n = 8); **c)** accumulation of [$^{64}$Cu]Cu-**2** in liver and intestine together as well as in kidney and urine together, at 5 min and 60 min p.i., respectively

Metabolic analysis showed that 2 h p.i. two main metabolites are present in kidney, to a smaller extent already in urine, and to an even smaller part also in liver and blood. The main radioactive peaks appeared to be unchanged [$^{64}$Cu]Cu-2 (**Fig. 7**).

**Fig. 7** HPLC profiles of [$^{64}$Cu]Cu-**2** meatabolites in blood, urine, kidney and liver samples, at 2h p.i. of 15 MBq [$^{64}$Cu]Cu-**2** (500 µL, 5% ethanol) compared to pure [$^{64}$Cu]Cu-**2** injection solution

Metabolic analysis of blood plasma yielded a decrease of original [$^{64}$Cu]Cu-**2** of about 15% 20 min after injection. 85% of [$^{64}$Cu]Cu-**2** was determined also at 60 and 120 min after injection like a plateau (**Fig. 8**).

**Fig. 8** Representative rat plasma acitivity curve of [$^{64}$Cu]Cu-**2** up to 120 min p.i. (15 MBq in 500 µL, 5% ethanol)

**Discussion**

NOTA was easily coupled with peptides via the isothiocyanate group. The resulting thiourea moiety displays high stability in buffer and serum (Lang et al. 2011; Shao et al. 2014; Kim et al.2015). NOTA peptide conjugates are steadily labeled with $^{64}$Cu at pH 6.2. Both linear and cyclic peptides were found to be stable in buffer and serum and displayed hydrophilic character. Inserting the linker between NOTA and the peptide no change of stability in buffer or serum as well as no influence on lipophilicity of the radiolabeled peptides was observed. Two isomers were detected for the linear $^{64}$Cu labeled NOTA peptides, because of the different conformation of the acid groups from NOTA when coordinating to $^{64}$Cu (Schlesinger et al. 2011). Considering the rapid isomeric conversion (within 10 min), after routine labeling, for biologic applications no separation was performed. The isomeric ratio was found to be constant between 1:7 and 1:11.

Competition studies were performed using the standard peptide [$^{125}$I]NDP-MSH. Based on $K_d$ and on the concentration of the standard, $K_i$ values were calculated to obtain concentration-independent values comparable with values from other studies. Results of affinity assays with α-MSH derivatives from other research groups were mainly presented as $IC_{50}$. This of course gives a tendency about high or low affinity, however, it is not directly comparable with values from different studies.

The murine B16F10 was used as gold standard for a MC1R expressing cell line to compare data with other studies. However, this study primarily aims at characterization of binding in MC1R expressing human melanoma cells, MeWo and TXM13, in order to identify an appropriate mouse xenograft model for further studies. There are five MCR subtypes, MC1 to MC5). It has been asserted that only the MC1R subtype occurs in melanocytes and is about 10 to 20 times higher expressed in melanoma tissue and cultured melanoma cells (Siegrist and Eberle 1995; Loir et al. 1999) than in healthy skin tissue.

Low MC1R expression has been found also in the adrenal glands, hepatocytes, and cortical neurons of the cerebellum (Salazar-Onfray et al. 2002). However, even if the standard [$^{125}$I]NDP-MSH peptide derived from α-MSH shows no selectivity when comparing binding affinity to MC1, MC3, MC4 and MC5 receptors (Schiöth et al. 1996; Kopanchik et al. 2005), it is a worthwhile pharmaceutical lead for development of appropriate MC1R peptides due to the overexpression of this receptor in melanomas. The MC2R subtype possesses less than 50% amino acid homology with the other MCRs and does not bind α-MSH peptides (Schiöth et al. 1996).

In all cell lines, the measured $K_d$ values of [$^{125}$I]NDP-MSH are in reasonably agreement with $K_d$ values reported in the literature (Siegrist et al. 1988, 1989, 1996; Eberle et al. 1991; Lunec et al. 1992; Chluba-de Tapia et al. 1996; Schiöth et al. 1998; Ringholm et al. 2004). There was a tendency for [$^{125}$I]NDP-MSH to exhibit slightly lower affinity in human melanoma cells MeWo and TXM13 compared to murine B16F10 cells. Compared to the three NAPamides investigated, unlabeled NDP-MSH had the highest affinity not only in the murine cell line, as found formerly (Chen et al. 2000), but also in the human cells.

Interestingly, after NOTA-conjugation to no linker linear peptide, the affinity was not changed as well as after metalation with $^{nat}$Cu or $^{64}$Cu. NAPamids, that have been investigated before, also showed high affinity but after conjugation with DOTA some loss was recorded (Froidevaux et al. 2004, 2005). However, in the present study, a slight decrement of affinity was observed after conjugating the εAhx-β-Ala-linker to the linear peptide, and clear affinity loss was measured after conjugation of the cyclic peptide and even more after $^{nat}$Cu insertion. A slight affinity decrease has also been observed when $^{nat}$Cu was inserted to the DOTA-NAPamide (Cheng et al. 2007) confirming this tendency of affinity decrease after $^{nat}$Cu inclusion into the NOTA-NAPamides. However, among the tested compounds, $^{nat}$Cu-**1** (no linker) did not show affinity change suggesting that the εAhx-β-Ala linker influenced the binding capability of the peptide. In the study from Froidevaux et al. (2004) two DOTA-NAPamides derivatives were compared whereby the NAPamide with DOTA on the Lys$^{11}$ showed higher affinity than the β-Ala$^3$ coupled DOTA-NAPamide. The ε-Ahx-β-Ala$^3$ coupled NOTA-NAPamide without the terminal Lys$^{11}$ (**2**) was similar affine as the DOTA-Lys$^{11}$ coupled one (Cheng et al. 2007; Bapst et al. 2007).

Considering the cyclized peptides, rhenium-cyclized α-MSH derivatives had affinities in the subnanomolar (Cheng et al. 2004) and low nanomolar range (Giblin et al. 1998; Cheng et al. 2002;

Miao et al. 2003) whereas assays with NAP-NS2 and its conjugates yielded in $K_i$ values > 10 nM. Similar to the NAP-NS2 conjugates DOTA-GMSH (Lim et al. 2012), a cyclic HYNIC α-MSH (Garcia et al. 2014), and β-Ala-Nle-cyclic α-MSH derivatives (Guo et al. 2010; Morais et al. 2013) are based on melanotan II nevertheless exhibited MC1R affinities higher than NAP-NS2. There are many possibilities to investigate exchange, adding or removing of amino acids within an α-MSH peptide as well as couple different linkers that result in steric, polarity or charge effects and thus influencing the binding to the MC1R. Since the NAP-NS1 and NAP-NS2 coupled with ε-Ahx-β-Ala linker were established as basic MSH derivatives in this study and the linear NAP-NS1 conjugate displayed higher affinity on murine melanoma cells, the $^{64}$Cu-labeled linear ε-Ahx-β-Ala-NOTA-NAP-NS1 (**2**) was applied in further assays such as binding kinetics and saturation on human melanoma cells.

Association and dissociation of [$^{64}$Cu]Cu-**2** binding in B16F10 cells was rather fast, at least the association course appeared similar as the [$^{125}$I]NDP-MSH binding association in MC1R expressing cells whereby its dissociation course was not complete (only 40%) [**Error! Bookmark not defined.**]. The time course of [$^{125}$I]NDP-MSH was described to be slightly slower (Siegrist et al. 1988; Tatro et al. 1990).

The high affinity of [$^{125}$I]NDP-MSH at MC1Rs was observed in several studies (Tatro et al. 1990; Schiöth et al. 1998; Kopanchuk et al. 2005), however, affinities in the low nanomolar range obtained with the $^{64}$Cu-labeled NAPamides investigated are sufficient with regard to imaging. The $B_{max}$ values of the labeled peptides investigated were not consistent. Thus, the linker in [$^{64}$Cu]-**2** might have a steric influence, in the same manner as in the cyclic variant [$^{64}$Cu]-**3**.

The human metastatic cell line MeWo have been shown to express MC1Rs clearly (Funasaka et al. 1999) and was applied as orthotopic tumor mouse model (Petrangolini et al. 2003). For TXM13 cells a rather high amount of MC1Rs was determined compared to other human melanoma cell lines (Siegrist et al. 1989; Miao et al. 2003), however in B16F10 even about 20.000 binding sites per cell were found (Cheng et al. 2007). The affinity of [$^{125}$I]I-NDP-MSH was in the same order of magnitude in B16F10 and the human cells comparable with former data, where also a low specific binding part was determined in human melanoma cells (Siegrist et al. 1989). The $K_d$ values of [$^{64}$Cu]-**2** were in the same range for murine and for human cells.

Data of biodistribution confirmed that the major excretion pathway of [$^{64}$Cu]-**2** is the kidney as it was determined from many studies before (Froidevaux et al. 2004; Chen et al. 2001; Cheng et al. 2002;

Miao et al.2002; Bapst et al. 2009). In the present study, fortunately a radioactivity reduction of two-third was observed in the kidney after 60 min p.i. Uptake in the kidney has to be concerned seriously since it is a dose-limiting organ for investigations with radiotracers because nephrotoxicity is not to be unterestimated especially regarding to targeted radiotherapy. After filtration by the glomerulus and reabsorption by the tubular cells low-molecular proteins and peptides will be delivered to renal lysosomes and metabolized after hydrolyzation (Maak et al. 1979). Thus, final radioactive metabolites do not leave the lysosomes quickly (Behr et al. 1998). It has been shown, that the nonspecific kidney accumulation after injection of radiolabeled MSH derivatives can be reduced significantly by coinjection of L-lysine (Froidevaux et al. 2004; Chen et al. 2000; Flook et al. 2013). Furthermore, negatively charged MSH peptides contribute as well to a decreased kidney retention (Behr et al. 1998). Probably, tubular reabsorption is facilitated by ionic interactions between positively charged peptides and negatively charged surfaces of proximal tubular cells, implying that renal uptake gets higher with positively charged peptides (Froidevaux et al. 2005). Thus, [$^{64}$Cu]-**2** of present study has a charge of -1 for chelate unit, presenting moderate low kidney uptake. For comparison we obtained for the kidney 5.9 ± 1.0 and 2.0 ± 0.3 % ID/g when determined 5 min and 60 min, respectively, after injection of [$^{64}$Cu]-**2**. This was much lower as found for a [$^{64}$Cu]Cu-DOTA-NAPamide (Cheng et al. 2007) where the chelator was conjugated on the N-terminal; moreover, [$^{64}$Cu]-**2** includes the β-alanine linker that might have an influence especially also for the liver uptake that was higher as well in the study of Chen et al. (2007). However, the referred studies were performed in mice. Presumably, depending on the position of the chelator and/or coupling of a linker NAPamide derivatives show higher or lower kidney accumulation, but mainly low liver uptake (Froidevaux et al. 2004; Bapst et al. 2009; Froidevaux et al. 2002). Labeling with $^{18}$F also showed rather moderate kidney accumulation, but unfortunately low tumor uptake (Cheng et al. 2007a). The cyclic variations of MSH conjugates in general present a higher kidney accumulation than the linear NAPamides (Behr et al. 1998; Chen et al. 2000; Cheng et al. 2004a; Guo et al. 2009, 2009a; Eberle et al. 2010). However, a $^{64}$Cu labeled cyclic NOTA conjugate showed lower moderate kidney uptake and improved tumor accumulation compared to the same cyclic peptide conjugated with DOTA (Guo and Miao 2012). The NOTA-NAPamide with DOTA at Lys$^{11}$ position was assumed to degrade to a main metabolite H-Lys([$^{111}$In]DOTA)-$NH_2$ found in mice urine (Flook et al. 2013).

Based on the receptor non-selective α-MSH analog NDP-MSH (Kopanchuk et al. 2005) and also the

investigated derivatives have not been presented as MC1R selective peptides. However, even MC1Rs were found to be overexpressed in melanoma, the peptides pass the excretion pathway through the kidney that was found to express low levels of MC1R, MC3R, MC4R and MC5R, in human, mouse or rat kidney (Ni et al. 2006; Si et al. 2013; Lindskog et al. 2014). Several studies showed that the uptake of the radiolabeled MSH derivatives could be blocked in the respective tumor after additional application of a non-labeled MSH analog. At the same time the studies present mainly no significant change of the update data for kidney after treatment with 'cold' MSH analogs (Gercia et al. 2014; Cheng et al. 2007a; Guo et al. 2012). In the study of Froidevaux et al. (Froidevaux et al. 2004) the kidney uptake decreased by about 25%, but increased kidney uptake was measured in the study of Cheng et al. (2007). Thus, it is suggested that at least the decrease of uptake in the tumor is MC1R related. Whereas in kidney the MCR expression is too low. However a more MC1R selective α-MSH peptide could be useful in the future.

## Conclusions

In this study, we investigated the pharmacological behavior of a linear α-MSH peptide with and without linker and chelator and a cyclic α-MSH peptide with linker and chelator. The cyclic peptide exhibited a bit higher hydrophilicity than the linear peptides, while binding affinity to MC1R of the cyclic peptide and modifications was lower than that of the linear peptides. Coupling the linker to the peptide had negligible influence on in vitro pharmacological behavior. [$^{64}$Cu]Cu-**1**, [$^{64}$Cu]Cu-**2** and [$^{64}$Cu]Cu-**3** were stable in buffer and serum. [$^{64}$Cu]Cu-**2** revealed rapid cellular association and dissociation in murine cells. Linear peptide derivatives showed high binding affinities on murine B16F10 cells as well as on human MeWo and TXM13 cells. Fewer binding sites were observed on human MeWo cells. Rat biodistribution of [$^{64}$Cu]Cu-**2** confirmed a reasonable renal excretion pathway. Two main metabolites were found in the kidney 2h after application. In the plasma about 85% of originally compound was still determined 1h and 2h after injection. Definitely, [$^{64}$Cu]Cu-**2** should be used for further pharmacokinetic studies on tumor bearing mice with regard to a future application in human to diagnose melanoma.

## Compliance with ethical standards

***Ethical approval*** The animal experiments were performed in accordance to the guidelines of the

German Regulations of Animal Welfare. The protocol was approved by the local Ethical Committee for Animal Experiments (reference number 24-9168.21-4/2004-1).

***Conflict of interest*** The authors declare that they have no conflict of interest.

## References


American Cancer Society (2015) Cncer Facts & Figures. http://www.cancer.org/acs/groups/content/@editorial/documents/document/acspc-044552.pdf. Assessed 13 January 2015

Ashton H, Millman JE, Telford R, Thompson JW, Davies TF, Hall R, Shuster S, Thody AJ, Coy DH, Kastin AJ (1977) Psychopharmacological and endocrinological effects of melanocyte stimulating hormones in normal man. Psychopharmacology 55:165-172

Bapst JP, Froidevaux S, Calame M, Tanner H, Eberle AN (2007) Dimeric DOTA-alpha-melanocyte-stimulating hormone analogs: synthesis and in vivo characteristics of radiopeptides with high in vitro activity. J Recept Signal Transduct Res 27:383-409

Bapst JP, Calame M, Tanner H, Eberle AN (2009) Glycosylated DOTA-alpha-melanocyte-stimulating hormone analogues for melanoma targeting: influence of the site of glycosylation on in vivo biodistribution. Bioconjug Chem 20:984-993

Behr TM, Goldenberg DM, Becker W (1998) Reducing the renal uptake of radiolabeled antibody fragments and peptides for diagnosis and therapy: present status, future prospects and limitations. Eur J Nucl Med 25:201-112

Biondi B, Bolzati C, Carta D, Salvarese N, Refosco F, Calderan A, Ruzza P (2010) The [Tc(N)PNP] metal fragment labeled peptide for MC1 receptors imaging: preliminary studies. J Peptide Sci 16(Suppl 1):182

Castrucci AM, Hadley ME, Sawyer TK, Hruby VJ (1984) Enzymological studies of melanotropins. Comp Biochem Physiol B 78:519-524

Chen J, Cheng Z, Hoffman TJ, Jurisson SS, Quinn TP (2000) Melanoma-targeting properties of (99m)technetium-labeled cyclic alpha-melanocyte-stimulating hormone peptide analogues. Cancer Research 60:5649-5658

Chen J, Cheng Z, Owen NK, Hoffman TJ, Miao Y, Jurisson SS, Quinn TP (2001) Evaluation of an (111)In-DOTA-rhenium cyclized alpha-MSH analog: a novel cyclic-peptide analog with improved tumor-targeting properties. J Nucl Med 42:1847-1855

Chen JQ, Cheng Z, Miao YB, Jurisson SS, Quinn TP (2002) Alpha-melanocyte- stimulating hormone peptide analogs labeled with technetium-99m and indium-111 for malignant melanoma targeting. Cancer 94(4 Suppl):1196-1201

Cheng Z, Chen J, Miao Y, Owen NK, Quinn TP, Jurisson SS (2002) Modification of the structure of a metallopeptide: synthesis and biological evaluation of (111)In-labeled DOTA-conjugated rhenium-cyclized alpha-MSH analogues. J Med Chem 45:3048-3056

Cheng Z, Chen J, Quinn TP, Jurisson SS (2004) Radioiodination of rhenium cyclized alpha-melanocyte-stimulating hormone resulting in enhanced radioactivity localization and retention in melanoma. Cancer Res 64:1411-1418

Cheng Z, Chen J, Quinn TP, Jurisson SS (2004a) Radioiodination of rhenium cyclized alpha-melanocyte-stimulating hormone resulting in enhanced radioactivity localization and retention in melanoma. Cancer Res 64:1411-1418

Cheng Z, Xiong ZM, Subbarayan M, Chen XY, Gambhir SS (2007) Cu-64-labeled alpha-melanocyte-stimulating hormone analog for MicroPET imaging of melanocortin 1 receptor expression. Bioconjug Chem 18:765-772

Cheng Z, Zhang L, Graves E, Xiong Z, Dandekar M, Chen X, Gambhir SS (2007a) Small-animal PET of melanocortin 1 receptor expression using a 18F-labeled alpha-melanocyte- stimulating hormone analog. J Nucl Med 48:987-994

Chluba-de Tapia J, Bagutti C, Cotti R, Eberle AN (1996) Induction of constitutive melanogenesis in amelanotic mouse melanoma cells by transfection of the human melanocortin-1 receptor gene. J Cell Sci 109(Pt 8):2023-2030

Cooper MS, Ma MT, Sunassee K, Shaw KP, Williams JD, Paul RL, Donnelly PS, Blower PJ (2012) Comparison of (64)Cu-complexing bifunctional chelators for radioimmunoconjugation: labeling efficiency, specific activity, and in vitro/in vivo stability. Bioconjug Chem 23:1029-1039. doi: 10.1021/bc300037w

Eberle AN (1988) 10. Secretion, Distribution and inactivation of MSH. In: Eberle AN (ed) The melanotropins. Chemistry, physiology and mechanisms of action, 1st edn. Karger, Basel, pp 173-209

Eberle AN, Verin VJ, Solca F, Siegrist W, Küenlin C, Bagutti C, Stutz S, Girard J (1991) Biologically active monoiodinated alpha-MSH derivatives for receptor binding studies using human melanoma cells. J Recept Res 11:311-122

Eberle AN, Bapst JP, Calame M, Tanner H, Froidevaux S (2010) MSH radiopeptides for targeting melanoma metastases. Adv Exp Med Biol 681:133-142. doi: 10.1007/978-1-4419-6354-3_11

Fani M, Maecke HR (2012) Radiopharmaceutical development of radiolabelled peptides. Eur J Nucl Med Mol Imaging 39:S11-30. doi: 10.1007/s00259-011-2001-z

Flook AM, Yang J, Miao Y (2013) Evaluation of new Tc-99m-labeled Arg-X-Asp-conjugated α-melanocyte stimulating hormone peptides for melanoma imaging. Mol Pharm 10:3417-3424. doi: 10.1021/mp400248f

Froidevaux S, Calame-Christe M, Tanner H, Sumanovski L, Eberle AN (2002) A novel DOTA-alpha-melanocyte-stimulating hormone analog for metastatic melanoma diagnosis. J Nucl Med 43:1699-1706

Froidevaux S, Calame-Christe M, Schuhmacher J, Tanner H, Saffrich R, Henze M, Eberle AN (2004) A gallium-labeled DOTA-alpha-melanocyte-stimulating hormone analog for PET Imaging of melanoma metastases. J Nucl Med 45:116-123

Froidevaux S, Calame-Christe M, Tanner H, Eberle AN (2005). Melanoma targeting with DOTA-alpha-melanocyte-stimulating hormone analogs: structural parameters affecting tumor uptake and kidney uptake. J Nucl Med 46:887-895

Funasaka Y, Sato H, Chakraborty AK, Ohashi A, Chrousos GP, Ichihashi M (1999) Expression of proopiomelanocortin, corticotropin-releasing hormone (CRH), and CRH receptor in melanoma cells, nevus cells, and normal human melanocytes. J Investig Dermatol Symp Proc 4:105-109

Fung S, Hruby VJ (2005) Design of cyclic and other templates for potent and selective peptide alpha-MSH analogues.Curr Opin Chem Biol 9:352-358

Garcia MF, Zhang X, Gallazzi F, Fernandez M, Moreno M, Gambini JP, Porcal W, Cabral P, Quinn TP (2014) Evaluation of tricine and EDDA as Co-ligands for $^{99m}$Tc-labeled HYNIC-MSH analogs for melanoma imaging. Anticancer Agents Med Chem 15:122-130

Giblin MF, Wang N, Hoffman TJ, Jurisson SS, Quinn TP (1998) Design and characterization of alpha-melanotropin peptide analogs cyclized through rhenium and technetium metal coordination. Proc Natl Acad Sci U S A 95:12814-12818

Guo H, Yang J, Gallazzi F, Prossnitz ER, Sklar LA, Miao Y (2009) Effect of DOTA position on melanoma targeting and pharmacokinetic properties of $^{111}$In-labeled lactam bridge-cyclized alpha-melanocyte stimulating hormone peptide. Bioconjug Chem 20:2162-2168. doi: 10.1021/bc9003475

Guo H, Yang J, Shenoy N, Miao Y (2009a). Gallium-67-labeled lactam bridge-cyclized alpha-melanocyte stimulating hormone peptide for primary and metastatic melanoma imaging. Bioconjug Chem 20:2356-2363

Guo H, Yang J, Gallazzi F, Miao Y (2010) Reduction of the ring size of radiolabeled lactam bridge-cyclized alpha-MSH peptide, resulting in enhanced melanoma uptake. J Nucl Med 51:418-426

Guo H, Miao Y (2012) Cu-64-labeled lactam bridge-cyclized α-MSH peptides for PET imaging of melanoma. Mol Pharm 9:2322-2330. doi: 10.1021/mp300246j

Kim MH, Park JA, Woo SK, Lee KC, An GI, Kim BS, Kim KI, Lee TS, Kim CW, Kim KM, Kang JH, Lee YJ (2015) Evaluation of a $^{64}$Cu-labeled 1,4,7-triazacyclononane, 1-glutaric acid-4,7 acetic acid (NODAGA)- galactose-bombesin analogue as a PET imaging probe in a gastrin-releasing peptide receptor-expressing prostate cancer xenograft model. Int J Oncol 46:1159-1168. doi: 10.3892/ijo.2015.2832

Kopanchuk S, Veiksina S, Petrovska R, Mutule I, Szardenings M, Rinken A, Wikberg JE (2005) Co-operative regulation of ligand binding to melanocortin receptor subtypes: evidence for interacting binding sites. Eur J Pharmacol 512:85-95

Lang L, Li W, Guo N, Ma Y, Zhu L, Kiesewetter DO, Shen B, Niu G, Chen X (2011) Comparison study of [$^{18}$F]FAl-NOTA-PRGD2, [$^{18}$F]FPPRGD2, and [$^{68}$Ga]Ga-NOTA-PRGD2 for PET imaging of U87MG tumors in mice. Bioconjug Chem 22:2415-2422. doi: 10.1021/bc200197h

Lim JC, Hong YD, Kim JJ, Choi SM, Baek HS, Choi SJ (2012) Synthesis and biological evaluation of a novel (177)Lu-DOTA-[Gly(3)-cyclized(Dap(4), (d)-Phe(7), Asp(10))-Arg(11)]α-MSH(3-13) analogue for melanocortin-1 receptor-positive tumor targeting. Cancer Biother Radiopharm 27:464-472

Lin MJ, Mar V, McLean C, Wolfe R, Kelly JW (2014) Diagnostic accuracy of malignant melanoma according to subtype. Australas J Dermatol 55:35-42. doi: 10.1111/ajd.12121

Lindskog Jonsson A, Granqvist A, Elvin J, Johansson ME, Haraldsson B, Nyström J (2014) Effects of melanocortin 1 receptor agonists in experimental nephropathies. PLoS One 9:e87816. doi: 10.1371/journal.pone.0087816

Loir B, Pérez Sánchez C, Ghanem G, Lozano JA, García-Borrón JC, Jiménez- Cervantes C (1999) Expression of the MC1 receptor gene in normal and malignant human melanocytes. A semiquantitative RT-PCR study. Cell Mol Biol 1999;45:1083-1092

López MN, Pereda C, Ramírez M, Mendoza-Naranjo A, Serrano A, Ferreira A, Poblete R, Kalergis AM, Kiessling R, Salazar-Onfray F (2007) Melanocortin 1 receptor is expressed by uveal malignant melanoma and can be considered a new target for diagnosis and immunotherapy. Invest Ophthalmol Vis Sci 48:1219-1227

Lunec J, Pieron C, Thody AJ (1992). MSH receptor expression and the relationship to melanogenesis and metastatic activity in B16 melanoma. Melanoma Res 2:5-12

Maack T, Johnson V, Kau ST, Figueiredo J, Sigulem D (1979) Renal filtration, transport, and metabolism of low-molecular-weight proteins: a review. Kidney Int. 16:251-270

Miao Y, Owen NK, Whitener D, Gallazzi F, Hoffman TJ, Quinn TP (2002) In vivo evaluation of 188Re-labeled alpha-melanocyte stimulating hormone peptide analogs for melanoma therapy. Int J Cancer 101:480-487

Miao Y, Whitener D, Feng W, Owen NK, Chen J, Quinn TP (2003) Evaluation of the human melanoma targeting properties of radiolabeled alpha-melanocyte stimulating hormone peptide analogues. Bioconjug Chem 14:1177-1184

Miao Y, Gallazzi F, Guo H, Quinn TP (2008) In-111-labeled lactam bridge-cyclized alpha-melanocyte stimulating hormone peptide analogues for melanoma imaging. Bioconjug Chem 19:539-547. doi: 10.1021/bc700317w

Morais M, Oliveira BL, Correia JD, Oliveira MC, Jiménez MA, Santos I, Raposinho PD (2013) Influence of the bifunctional chelator on the pharmacokinetic properties of $^{99m}Tc(CO)_3$-labeled cyclic α-melanocyte stimulating hormone analog. J Med Chem 56:1961-1973. doi: 10.1021/jm301647t

Ni XP, Bhargava A, Pearce D, Humphreys MH (2006) Modulation by dietary sodium intake of melanocortin 3 receptor mRNA and protein abundance in the rat kidney. Am J Physiol Regul Integr Comp Physiol 290:R560-R567

Petrangolini G, Pratesi G, De Cesare M, Supino R, Pisano C, Marcellini M, Giordano V, Laccabue D, Lanzi C, Zunino F (2003) Antiangiogenic effects of the novel camptothecin ST1481 (gimatecan) in human tumor xenografts. Mol Cancer Res 1:863-870

Raposinho PD, Xavier C, Correia JDG, Falcao S, Gomes P, Santos I (2008) Melanoma targeting with alpha-melanocyte stimulating hormone analogs labeled with fac-[Tc-99m(CO)(3)](+): effect of cyclization on tumor-seeking properties. J Biol Inorgan Chem 13:449-459. doi: 10.1007/s00775-007-0338-3

Ringholm A, Klovins J, Rudzish R, Phillips S, Rees JL, Schiöth HB (2004) Pharmacological characterization of loss of function mutations of the human melanocortin 1 receptor that are associated with red hair. J Invest Dermatol 123:917-923

Rudman D, Hollins BM, Kutner MH, Moffitt SD, Lynn MJ (1983) Three types of alpha-melanocyte-stimulating hormone: bioactivities and half-lives. Am J Physiol 245:E47-54

Salazar-Onfray F, López M, Lundqvist A, Aguirre A, Escobar A, Serrano A, Korenblit C, Petersson M, Chhajlani V, Larsson O, Kiessling R (2002) Tissue distribution and differential expression of melanocortin 1 receptor, a malignant melanoma marker. Br J Cancer 87:414-422

Sawyer TK, Sanfilippo PJ, Hruby VJ, Engel MH, Heward CB, Burnett JB, Hadley ME (1980) 4-Norleucine, 7-D-phenylalanine-alpha-melanocyte-stimulating hormone: a highly potent alpha-melanotropin with ultralong biological activity. Proc Natl Acad Sci U S A 77:5754-5758

Schiöth HB, Chhajlani V, Muceniece R, Klusa V, Wikberg JE (1996) Major pharmacological distinction of the ACTH receptor from other melanocortin receptors. Life Sci 59:797-801

Schiöth HB, Yook P, Muceniece R, Wikberg JE, Szardenings M (1998) Chimeric melanocortin MC1 and MC3 receptors: identification of domains participating in binding of melanocyte-stimulating hormone peptides. Mol Pharmacol 54:154-161

Schlesinger J, Rajander J, Ihalainen JA, Ramesh D, Eklund P, Fagerholm V, Nuutila P, Solin O (2011) Isomerism of [64Cu-NOTA-Bn]-labeled radiotracers: separation of two complex isomers and determination of their interconversion energy barrier using ion pair chromatography. Inorg Chem 50:4260-4271. doi: 10.1021/ic101775q

Schottelius M, Wester HJ (2009) Molecular imaging targeting peptide receptors. Methods 48:161-177. doi: 10.1016/j.ymeth.2009.03.012

Shao Y, Liang W, Kang F, Yang W, Ma X, Li G, Zong S, Chen K, Wang J (2014). $^{68}$Ga-labeled cyclic NGR peptide for microPET imaging of CD13 receptor expression. Molecules 19:11600-12. doi: 10.3390/molecules190811600

Si J, Ge Y, Zhuang S, Wang LJ, Chen S, Gong R (2013) Adrenocorticotropic hormone ameliorates acute kidney injury by steroidogenic-dependent and -independent mechanisms. Kidney Int 83:635-646. doi: 10.1038/ki.2012.447

Siegrist W, Oestreicher M, Stutz S, Girard J, Eberle AN (1988) Radioreceptor assay for alpha-MSH using mouse B16 melanoma cells. J Recept Res 8:323-343

Siegrist W, Solca F, Stutz S, Giuffre L, Carrel S, Girard J, Eberle AN (1989) Characterization of Receptors for Alpha-Melanocyte-Stimulating Hormone on Human-Melanoma Cells. Cancer Research 49:6352-6358

Siegrist W, Eberle AN (1995) Melanocortins and their implication in melanoma.Trends Endocrinol Metab 6:115-120

Siegrist W, Willard DH, Wilkison WO, Eberle AN (1996) Agouti protein inhibits growth of B16 melanoma cells in vitro by acting through melanocortin receptors. Biochem Biophys Res Commun 218:171-175

Tandler N, Mosch B, Pietzsch J (2012) Protein and non-protein biomarkers in melanoma: a critical update. Amino Acids 43:2203-2230. doi: 10.1007/s00726-012-1409-5

Tatro JB, Entwistle ML, Lester BR, Reichlin S (1990) Melanotropin receptors of murine melanoma characterized in cultured cells and demonstrated in experimental tumors in situ. Cancer Res 50:1237-1242

Yang J, Guo H, Padilla RS, Berwick M, Miao Y (2010) Replacement of the Lys linker with an Arg linker resulting in improved melanoma uptake and reduced renal uptake of Tc-99m-labeled Arg-Gly-Asp-conjugated alpha-melanocyte stimulating hormone hybrid peptide. Bioorg Med Chem 18:6695-6700

Figure

Click here to download Figure Fig1.tif

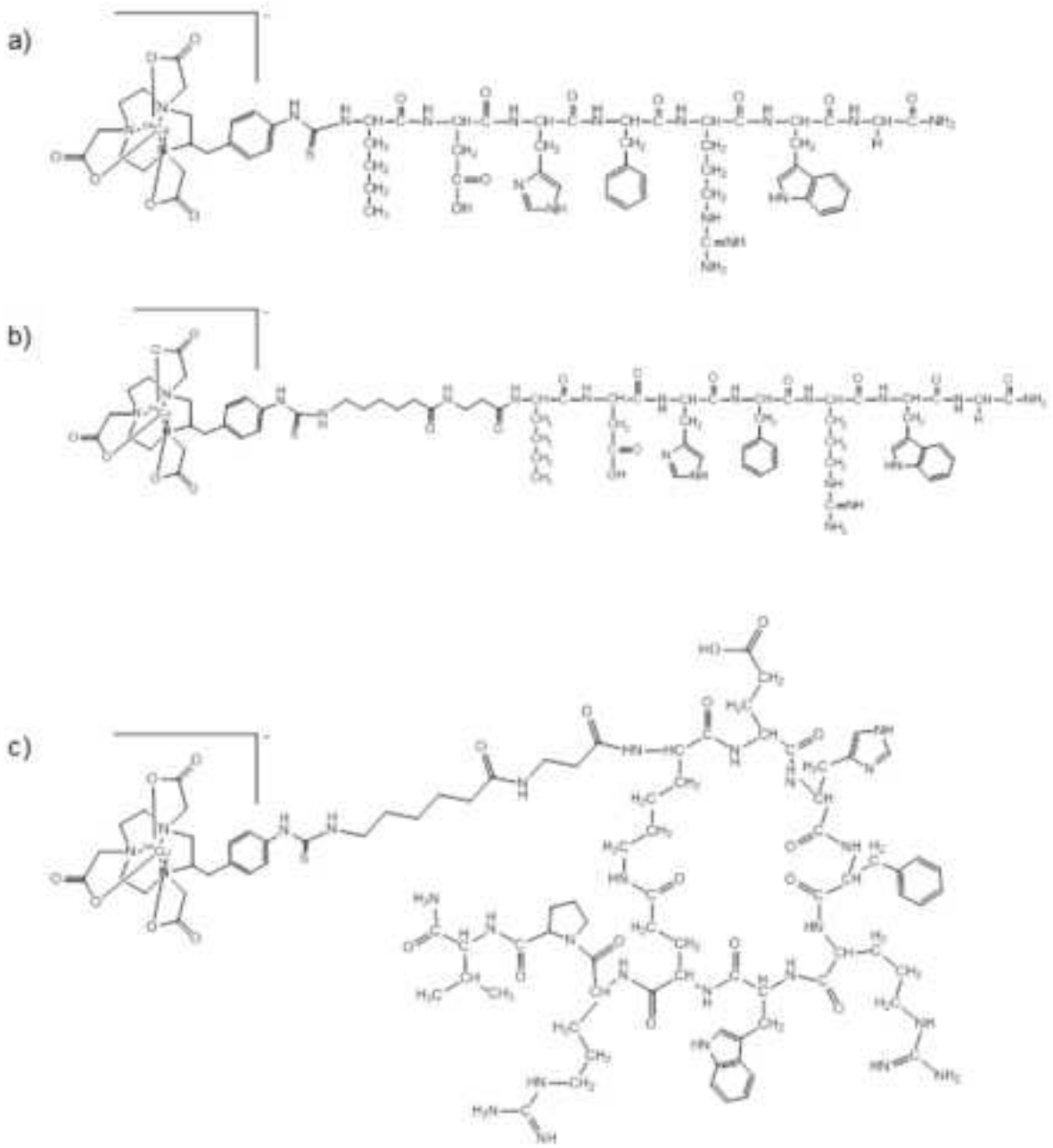

Figure

Click here to download Figure Fig2.tif

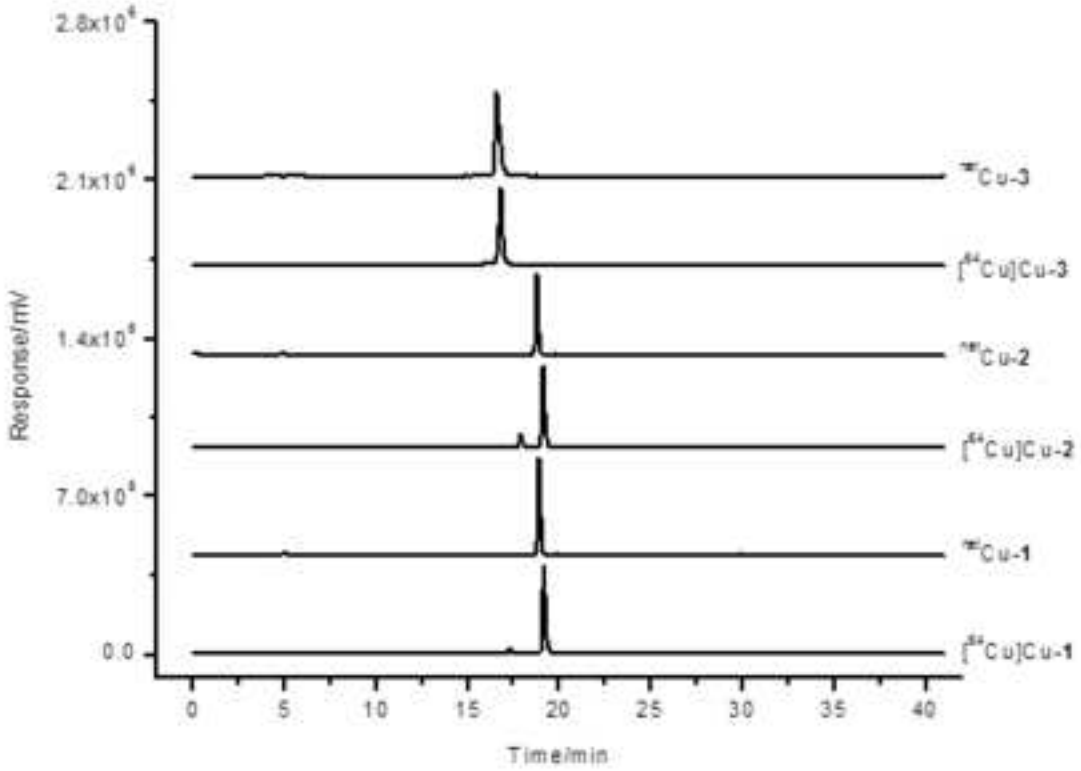

Figure

Click here to download Figure Fig3.tif

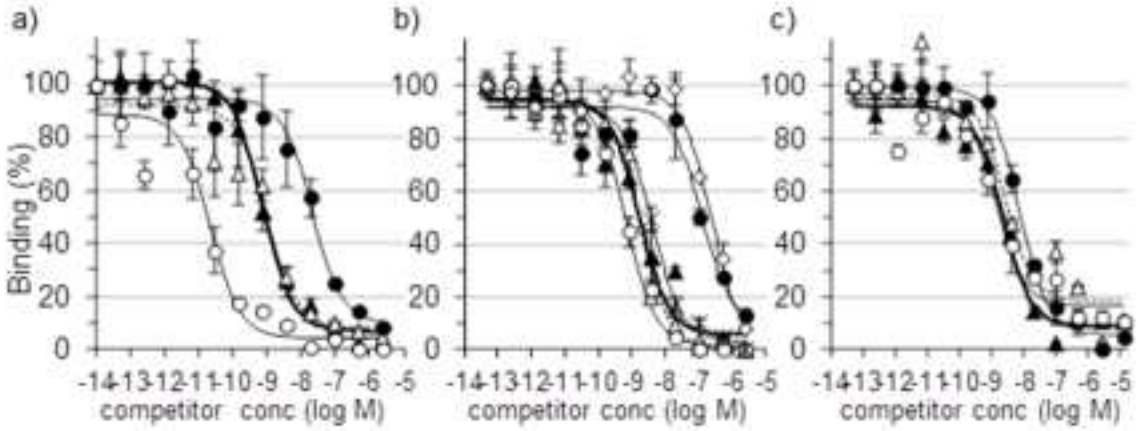

Figure

Click here to download Figure Fig4.tif

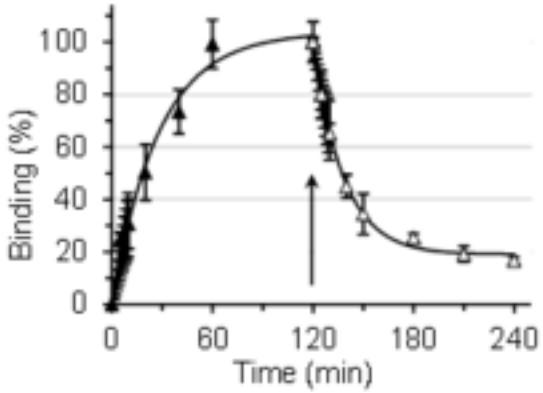

Figure

Click here to download Figure Fig5.tif

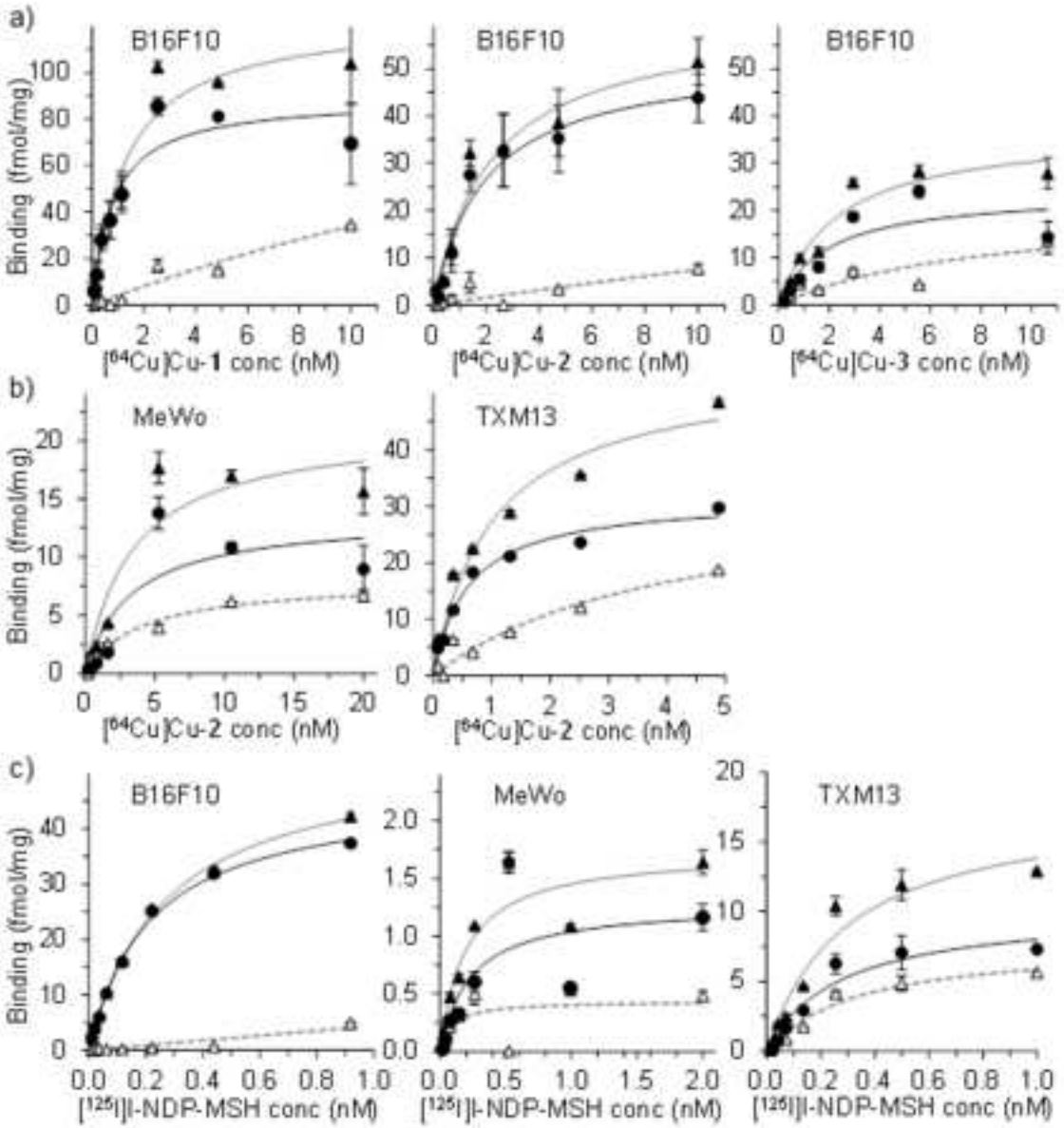

Figure

Click here to download Figure Fig6.tif

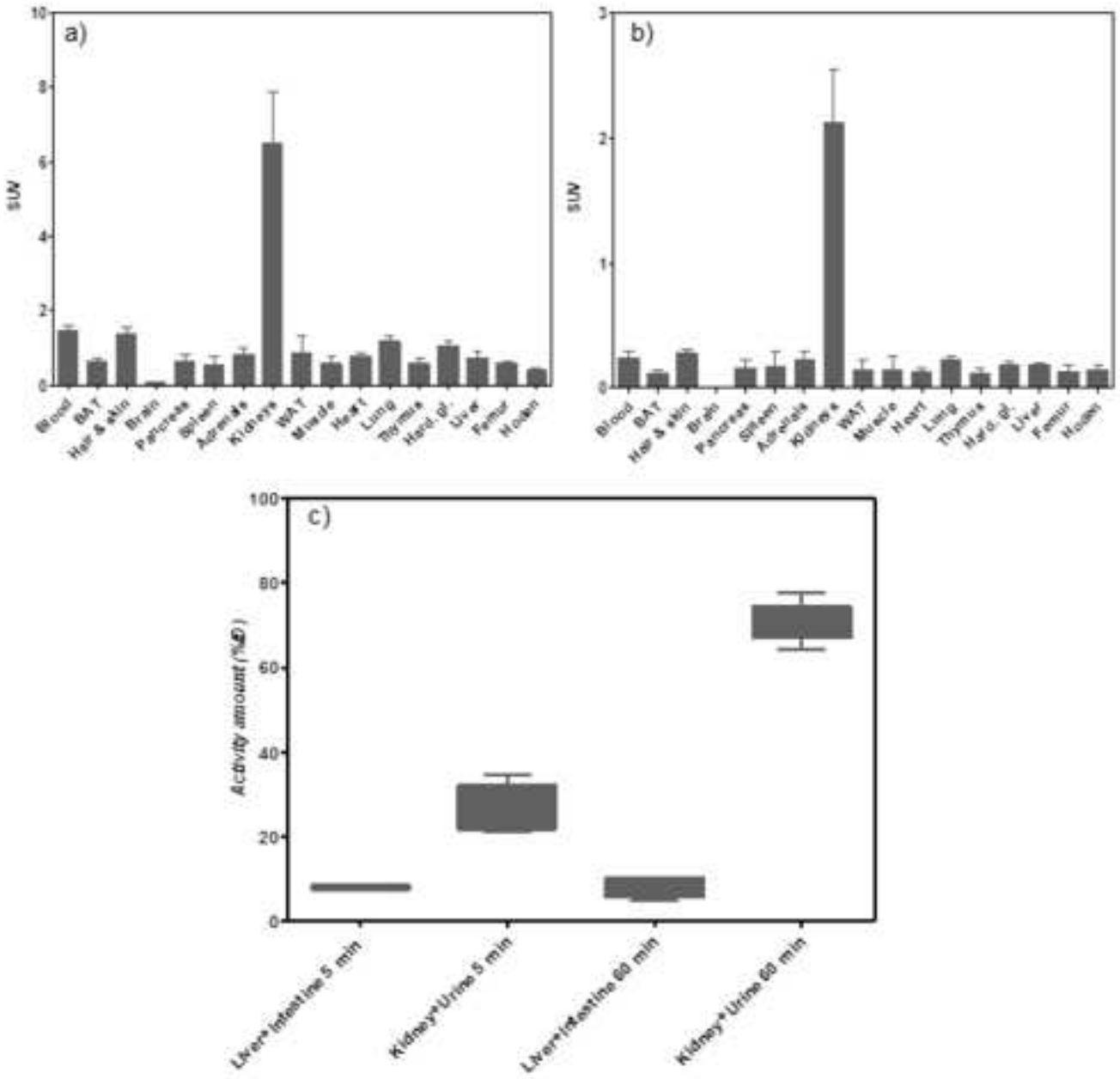

Figure

Click here to download Figure Fig7.tif

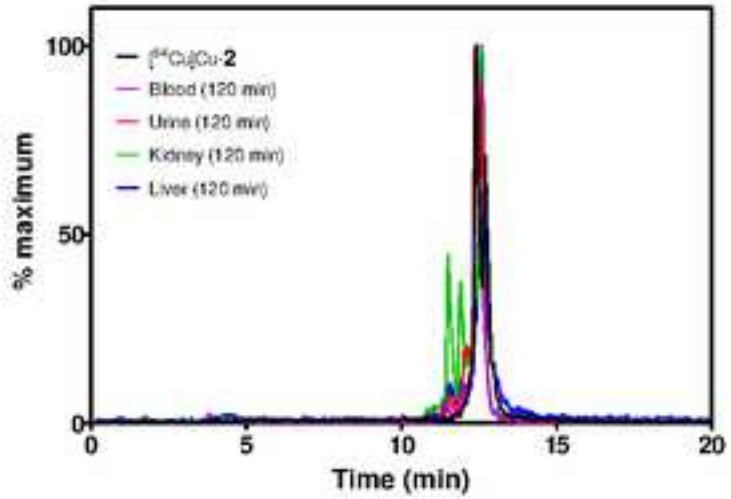

Figure

Click here to download Figure Fig8.tif